

P. Papakonstantinou¹ · J.W. Clark²

Three-nucleon forces and superfluidity in neutron matter

the date of receipt and acceptance should be inserted later

Abstract The existence of superfluidity of the neutron component in the core of a neutron star, associated specifically with triplet P-wave pairing, is currently an open question that is central to interpretation of the observed cooling curves and other neutron-star observables. *Ab initio* theoretical calculations aimed at resolving this issue face unique challenges in the relevant high-density domain, which reaches beyond the saturation density of symmetrical nuclear matter. These issues include uncertainties in the three-nucleon (3N) interaction and in the effects of strong short-range correlations – and more generally of in-medium modification of nucleonic self-energies and interactions. A survey of existing solutions to the gap equations in the triplet channel shows that the separate or combined impacts of 3N forces, coupled channels, and mass renormalization range from moderate to strong to devastating, thus motivating a detailed analysis of the competing effects. In the present work we track the effects of the 3N force and in-medium modifications in the representative case of the 3P_2 channel, based on the Argonne V18 two-nucleon (2N) interaction supplemented by 3N interactions of the Urbana IX family. Sensitivity of the results to the input interaction is clearly demonstrated, while consistency issues arise with respect to the simultaneous treatment of 3N forces and in-medium effects. We consider this pilot study as the first step towards a systematic and comprehensive exploration of coupled-channel $^3P_{F_2}$ pairing using a broad range of 2N and 3N interactions from the current generation of refined semi-phenomenological models and models derived from chiral effective field theory.

Keywords Nuclear superfluidity · Neutron stars · Nuclear forces · BCS gap equations

¹Rare Isotope Science Project, Institute for Basic Science,
Daejeon 34047, Republic of Korea
E-mail: ppapakon@ibs.re.kr

²McDonnell Center for the Space Sciences and Department of Physics, Washington University,
St. Louis, MO 63130, USA
E-mail: jwc@wuphys.wustl.edu

1 Introduction

Nucleonic systems demonstrate superfluid and superconducting properties in a variety of density and composition regimes [1]. Odd-even staggering served historically as the first clue to the presence of superfluidity in finite nuclei, while rotational spectra exhibit the effect of superfluidity on the nuclear moments of inertia. The formation and properties of neutron halos in light drip-line nuclei, currently under investigation theoretically and in modern radioactive-beam facilities, are also influenced by pairing. Neutron stars serve as rich laboratories for nuclear-matter studies across a vast range of densities. Cooling via neutrino emission, glitches, and rotational dynamics are all sensitive to the pairing strength in different two-nucleon channels and for different isospin compositions [2, 3]. In particular, the presence of nucleonic superfluidity and the magnitude of the pairing gap in the homogeneous hadronic phase present in the outer core of a neutron star is an open question, whose answer is pivotal for interpretation of the observed cooling data [4, 5, 6].

Unlike electronic systems in terrestrial solids, where the pairing mechanism depends on the presence of an ionic lattice, the attractive force generating pairing in nuclear systems comes directly from the interactions between and among the nucleons themselves. These interactions, possessing both attractive and repulsive components, exhibit rich operatorial structure expressing complicated dependence on space, spin, and isospin, giving rise to diverse and subtle pairing phenomena. At the most basic level, we may distinguish between isoscalar pairing, active in isospin-symmetric nuclei in the deuteron channel, and isovector pairing, especially relevant in halo nuclei and neutron-star matter. Next we may consider the partial-wave decomposition of the nucleon-nucleon interaction, with different angular momenta coming into play becoming more important at different relative energies, corresponding to different nucleonic densities. In particular, one may infer that singlet 1S_0 pairing of neutrons is active at subsaturation densities, i.e., in nuclear haloes and in the neutron fluid interpenetrating the rigid pasta-like structures that may be formed by the neutron-rich nuclei in the inner crust of a neutron star, while neutron pairing in higher partial waves, if present, affects only the dense hadronic liquid at greater depth in the star's outer core. In the latter case, the tensor interaction couples different angular-momentum channels, and anisotropic pairing gaps cannot be excluded, specifically in the triplet 3P_F state. Proton pairing in the 1S_0 channel is expected to occur in this same density region, where the partial density of the sparse proton admixture required for β -stability will be similar to that of neutrons in the inner crust.

There exist many calculations of the pairing gap in the singlet S -wave channel (for recent reviews and comparisons, see [6, 7, 8], and references cited therein). While different calculational methods have yielded a considerable spread of predicted values, there is a growing consensus that in pure neutron matter the gap value should reach a maximum of about 2 MeV at a Fermi momentum somewhat lower than 1 fm^{-1} . Results from many different approaches are compiled, for example, in Fig. 6 of Ref. [8]. In view of the extreme (nominally exponential) sensitivity of the pairing gap to the pairing interaction and the density of single-fermion states, the lack of quantitative agreement of the different microscopic approaches is not surprising.

In this contribution we focus on issues of the existence and intensity of pairing as it might occur in the liquid hadronic outer core of a neutron star, at densities ranging up to several times the saturation density of symmetrical nuclear matter, where triplet neutron pairing is most likely to occur. The theoretical challenges encountered under the extreme conditions in play abound and uncertainties accumulate. At such high densities, the 3N force, which reflects the composite nature of nucleons and is poorly constrained, cannot be neglected. Also inadequately controlled are significant short-range correlations and self-energy effects, whose treatment involves approximations of variable reliability.

It should be noted that the effect of the 3N force on the singlet- S pairing gap has been found to be quite minor, owing to the much lower density at which this gap reaches its peak value, occurring at a small fraction ($\sim 1/8 - 1/10$) of the saturation density of symmetrical nuclear matter. In theoretical calculations, this effect would be masked by other uncertainties involving medium-polarization and self-energy corrections [36, 30].

To set the context for our study, let us consider briefly the results of three previous calculations of the isospin $T = 1$ triplet gap at neutron-star densities that include a 3N interaction. For relevant earlier work on the 3P_2 pairing problem and its coupled-channel extension 3P_2F_2 , both theoretical and computational, see Refs. [9, 10, 11, 12, 13, 14, 15, 16, 17, 18, 19].

Contributing to the long-term effort of the Catania group on nucleonic pairing, W. Zuo et al. [20] employed the Argonne v_{18} (AV18) two-nucleon (2N) potential along with a modified Urbana IX (UIX) 3N interaction [21] in a study of 3P_2F_2 pairing in pure neutron matter. The parameters of the original UIX 3N potential were readjusted in order to obtain realistic results for saturation of symmetrical nuclear matter, as calculated within Brueckner-Hartree-Fock (BHF) theory [22]. The modified 3N potential is far less repulsive at short distances than the original version. The latter was developed by the Argonne-Urbana group with parameters which, in conjunction with the AV18 interaction, (i) reproduce the empirical saturation properties of symmetrical nuclear matter as calculated in the single-operator-chain version of variational many-body theory, while also (ii) yielding satisfactory consistency with three-nucleon binding. Inclusion, by Zuo et al., of an additional term in the pairing interaction corresponding to the modified UIX 3N interaction resulted in a substantial enhancement of the gap's maximal value over that obtained for the AV18 2N potential alone, namely about 0.7 MeV, to almost 1.2 MeV, at $k_F \approx 2.2\text{fm}^{-1}$. This result was obtained using a free single-particle spectrum in the denominator of the gap equation. Upon replacing the free spectrum by its Brueckner-Hartree-Fock counterpart so as to include some in-medium effects ("correlations"), the gap was reduced to about 0.5 MeV.

In a more recent study along similar lines, J. M. Dong et al. [23] utilized the Bonn B 2N potential, together with a meson-exchange 3N potential with the same meson parameters as Bonn B [24]. They found a strong enhancement of the gap and a shift of its peak position versus k_F when the 3N force was included. The result with the 3N force in effect showed a maximal value of the gap of about 0.6 MeV at $k_F \approx 2.3\text{fm}^{-1}$. When the effect of correlations was estimated in terms of the so-called Z -factor, which quantifies the depletion of the fermion occupation number around the Fermi surface, the gap was reduced by an order of magnitude to an insignificant maximal value of about 50 keV at $k_F \approx 1.8\text{fm}^{-1}$.

S. Maurizio et al. [25] considered chiral 2N and 3N potentials, including a high-precision 2N potential developed at next-to-next-to leading order in the chiral expansion. In a representative example, taking account of the 3N force resulted in a modest enhancement of the gap by some 20%, yielding a maximal gap of 1.15 MeV, close to the uncorrelated result of Ref. [20]. Inclusion of in-medium modifications of the effective mass reduced the gap by approximately one third to a maximal value about 0.35 MeV at $k_F \approx 2.2\text{fm}^{-1}$.

Based on the above survey, we infer that the combined effect of 3N forces and correlations on the results of calculations of the triplet pairing gap in neutron matter ranges from moderate to strong to devastating, depending on the precise inputs. Moreover, the effects of the three-nucleon force on one hand and correlations on the other can be both large and opposite.

Pointing to selected earlier investigations, it becomes apparent that the input 3N interaction itself, even if its choice must somehow be plausible, can quite readily either make or break a triplet gap found to be present for the 2N interaction alone. A microscopic 3N potential obeying certain consistency requirements with respect to the AV18 potential has been shown [29] to produce a weaker triplet-pairing gap in stellar matter than obtained by Zuo et al. [20] using the modified UIX interaction. On the other hand, use of the original UIX parameterization emphatically kills the gap at least in the uncoupled 3P_2 channel [30]. (We will follow up on this latter finding, in considerable detail.) It is important to note that all three of these versions of the 3N potential, when combined with the AV18 2N interaction, reproduce the empirical saturation properties of nuclear matter within specific (and competing) many-body methods. Accordingly, such disagreement in the solutions of triplet gap equations raises issues of consistency for the many-body theories *vis à vis* the interactions involved.

In the present work, the sensitivity of the results to the input interaction, sometimes dramatic, will be clearly demonstrated. Thus, one's control of the approximations involved, or rather the lack thereof, will be revealed. We introduce two novelties relative to the prevalent treatments of gap equations in the presence of a 3N interaction, which were proposed and originally implemented in Ref. [30]. First, we avoid the usual approximation of averaging the 3N interaction over the third (unpaired) particle to produce a density-dependent effective 2N interaction. Rather, we introduce the explicit 3N interaction when constructing the two-body pairing-interaction matrix elements in momentum space, for insertion into the gap equation. (This will introduce a term in the pairing matrix elements having an additional momentum integration over the unpaired neutron.) Second, along with results for the modified UIX potential, we obtain results with the original parameterization of the UIX potential which yields a proper equation of state within variational chain-summation methods [31] and predicts a neutron star mass-radius relation which is consistent within observational constraints [32, 33, 34].

The present exploration focuses on pure neutron matter and on the 3P_2 channel. The coupled-channel problem will be addressed in future work. The purpose at present is not to provide the most realistic predictions, but instead to trace the sensitivity of the results to the most basic inputs. As will be seen, already within this simplified model system the inclusion and parameterization of the 3N force is of supreme importance, and very basic questions arise for quantum many-body theory: What does a "consistent" treatment of the 3N interaction entail? Given

that the 3N interaction is already in a sense an in-medium effect, what additional in-medium effects must be considered and how? Such questions are especially pertinent in the era of *ab initio* nuclear structure, as pairing becomes a testing ground for modern chiral interactions [25].

The paper is organized as follows. In Sec. 2 we sketch the theoretical basis for our study, namely the BCS approach extended to triplet pairing, applied in angle-averaged approximation, and show baseline results for the triplet 3P_2 pairing gap. Importantly, we explain our treatment of the 3N interaction and the formulae pertinent to the implementation of the UIX potential. Our main results are presented in Sec. 3. In particular, Sec. 3.1 tracks the influence of the attractive part and the phenomenological repulsive part of the Urbana potential by varying the coupling constants. At first, kinetic energies are used for single-particle energies with the bare neutron mass, and no correlations or in-medium effects are considered, beyond those implicit at the BCS level. In Sec. 3.2 we discuss results based on an effective nucleon mass. Also in Sec. 3.2 we introduce a defect function to parameterize the correlations experienced by the third unpaired nucleon. In Sec. 3.3 the results are analyzed in terms of the overall nucleon-nucleon pairing potential near the Fermi surface. Conclusions are drawn and perspectives are given in Sec. 4.

2 BCS equations for three interacting nucleons and baseline results

2.1 Basic gap equations and numerical solution

Derivations of the BCS gap equations for isospin $T = 1$ triplet pairing can be found in several sources; for example, see Refs. [12, 14]). A suitable generalization of the BCS superfluid trial ground state for singlet pairing to the more complicated case of triplet pairing can take the form

$$|\Phi_s\rangle = \mathcal{N}^{-1} \prod_{\sigma\sigma'\mathbf{k},k_x>0} \left(1 + g_{\sigma\sigma'}(\mathbf{k})a_{\mathbf{k}\sigma}^\dagger a_{-\mathbf{k}\sigma}^\dagger\right) |0\rangle, \quad (1)$$

where $|0\rangle$ is the quasiparticle vacuum and \mathcal{N} is a normalization constant. The factor $g_{\sigma,\sigma'}(\mathbf{k})$, though a matrix, plays the role of a variational function, analogous to $h(\mathbf{k})$ of the original BCS derivation [26]. This state does not conserve the particle number $N = \langle \hat{N} \rangle = \langle \sum_{\mathbf{k}\sigma} a_{\mathbf{k}\sigma}^\dagger a_{\mathbf{k}\sigma} \rangle$. Consequently $g_{\sigma\sigma'}(\mathbf{k})$ is to be determined by functional minimalization of the expectation $\langle \hat{H} - \mu \hat{N} \rangle$ subject to the constraint of a constant quasiparticle density. Here \hat{H} is the Hamiltonian and μ is a Lagrange multiplier interpreted as the chemical potential. The resulting matrix analog of the BCS gap equation can be reduced by partial-wave analysis, leading to a set of gap equations in general coupled with one another, for gap components $\Delta_{\mathbf{k}}^{LSJM}$ belonging to specific spin/angular-momentum channels. Such partial-wave gap equations have been derived and studied extensively by Takatsuka and Tamagaki [14], and the equations for pairing in the 3PF_2 coupled-channel case have been analyzed in detail more recently by Khodel et al. [18, 19] based on a separation algorithm for their solution [35, 17].

At present we are concerned primarily with the uncoupled triplet channel 3P_2 . Upon averaging over angles and five components corresponding to the allowed M projections for $J = 2$, the angle-averaged 3P_2 gap function, henceforth denoted

simply as $\Delta(k)$, is found (cf. [30]) to obey an equation of the same form as that for the 1S_0 gap,

$$\Delta(k) = -\frac{1}{\pi} \int_0^\infty dk' k'^2 \frac{V(k, k') \Delta(k')}{\sqrt{[(\varepsilon_{\mathbf{k}'} - \mu)]^2 + [\Delta(k')]^2}}, \quad (2)$$

where $V(k, k')$ is the central part of the potential belonging to the given multipolarity, as represented in momentum space. Invoking the separation method [35, 17, 30], numerical solution for a given value of Fermi momentum k_F is facilitated by introducing certain functions $f(k)$, $\chi(k)$, and $W(k, k')$ through the definitions

$$\Delta(k) \equiv \Delta_F f(k), \quad \Delta_F \equiv \Delta(k_F), \quad (3)$$

$$V_F \equiv V(k_F, k_F), \quad \chi(k) \equiv V(k, k_F)/V_F, \quad (4)$$

$$W(k, k') \equiv V(k, k') - V_F \chi(k) \chi(k'). \quad (5)$$

Importantly, we note the property $W(k, k_F) = W(k_F, k) = 0$, which allows the gap equation for given k_F to be recast as the following system of two coupled equations:

$$f(k) + \frac{1}{\pi} \int_0^\infty dk' k'^2 \frac{W(k, k') f(k')}{\sqrt{[(\varepsilon_{\mathbf{k}'} - \mu)]^2 + [\Delta_F f(k')]^2}}, \quad (6)$$

$$\frac{V_F}{\pi} \int_0^\infty dk' k'^2 \frac{\chi(k') f(k')}{\sqrt{[(\varepsilon_{\mathbf{k}'} - \mu)]^2 + [\Delta_F f(k')]^2}} = -1. \quad (7)$$

The unknowns are Δ_F and $f(k)$. In fact, the single-particle energies $\varepsilon_{\mathbf{k}}$ and chemical potential μ are also unknown and should be determined self-consistently, greatly complicating the problem. Instead we shall assume that $\varepsilon(k)$ and μ are known within some approximation, as considered in Sec. 2.3. Solution then becomes rather straightforward: In an initial step, we set $\Delta_F f(k) = \delta_0$, a small constant, in the denominator of Eq. (6). This equation then becomes a standard Fredholm equation of the second kind with respect to $f(k)$ and can be solved using standard routines. Given $f(k)$, the root Δ_F of Eq. (7) can be found, for example, through bisection. The new Δ_F can be fed back into Eq. (6). Consistency is achieved quite fast in practice. Also, as a practical matter, the potential $V(k, k')$ need not be calculated on the fly. Rather, we store its values on a k -space mesh, in a file from which they can be read each time calculations need to be executed.

2.2 Three-nucleon gap equations

The derivation of the 3N gap equation is detailed in Ref. [30]. Here we outline the basic steps and assumptions. An important assumption is again the angle-average approximation, a partial-wave decomposition being implied. Here we consider only the triplet 3P_2 channel, without coupling to the 3F_2 channel.

The angle-averaging treatment has been commonly applied in previous numerical studies of triplet- P pairing in nucleonic media, as in Refs. [15, 17, 20]. It is well justified for two reasons. First, there exists a striking near-degeneracy of the energies of the five magnetic substates involved in the uncoupled 3P_2 problem, irrespective of the details of the interaction, i.e., such behavior is universal.

This property, having a sound theoretical basis, was discovered by Takatsuka and Tamagaki [10, 14] and validated unambiguously in more recent analyses [16, 17], that exploit the separation method for solving coupled gap equations. (The near-degeneracy is lifted somewhat by the tensor force acting in the $3PF_2$ coupled-channel case, where there exist thirteen real solutions, another universal property [18, 19]). The second reason is strategic: the angle-averaged gap is the quantity of most immediate importance in the astrophysical implications of the existence and strength of triplet- P pairing for neutron-star cooling.

Accordingly, we will be working with the 2N pairing potential $V(k, k')$ and an additional 3N pairing potential $V_3(k, k', k'')$, without angular dependencies. Thus two nucleons form a Cooper pair in the 3P_2 channel and a spectator nucleon can interact with them. Only 1S_0 interactions are assumed between the spectator and the other particles, higher partial waves being ignored at present, in an approximation we adopted from Ref. [36] that may require improvement at high densities. It turns out that the gap obeys Eq. (2) just as in the 2N case, with the difference that the two-body potential $V(k, k')$ entering the equation receives an additive contribution from the 3N potential that reads [30]

$$V^{(3)}(k, k') = \frac{1}{\pi} \int_0^\infty dk'' k''^2 V_3(k, k', k'') \times \int_{-1}^1 dx \left[1 - \frac{\varepsilon_{k''} - \mu}{\sqrt{(\varepsilon_{k''} - \mu)^2 + \frac{1+3x^2}{16\pi} [\Delta(k'')]^2}} \right] \quad (8)$$

$$\approx \frac{4}{\pi} \int_0^{k_F} dk'' k''^2 V_3(k, k', k'') \equiv V^{(3)}(k, k'; k_F). \quad (9)$$

(The indicated approximation, which is quite accurate, takes advantage of the smallness of the triplet gap relative to the Fermi energy corresponding to relevant k_F values [30].)

Finally, we give the expression for $V_3(k, k', k'')$ in the special case of an Urbana-type potential, consisting of an attractive two-pion exchange term of strength $A_{2\pi}$ and a phenomenological repulsion term of strength U_0 [30]:

$$V_3(k, k', k'') = \frac{1}{2kk'} \int d\tilde{r}_1 d\tilde{r}_2 dx k\tilde{r}_1 j_1(k\tilde{r}_1) \{ k'\tilde{r}_1 j_1(k'\tilde{r}_1) \tilde{r}_2^2 \times \{ 2A_{2\pi}[-6(Y_1 Y_2 + Y_3 Y_1) + \frac{12}{5}(T_1 Y_2 + Y_3 T_1) + 18Y_2 Y_3] + U_0[T_1^2 T_2^2 + T_2^2 T_3^2 + T_3^2 T_1^2] \} + (1 + 3x^2) \tilde{r}_1 \tilde{r}_2 j_0(k'' \tilde{r}_3) k' \tilde{r}_2 j_1(k' \tilde{r}_2) \times \{ 2A_{2\pi}[2Y_1 Y_2 - 6(Y_2 Y_3 + Y_3 Y_1) + \frac{12}{5}(T_2 Y_3 + Y_3 T_1) - \frac{4}{5}(Y_1 T_2 + T_1 Y_2) + \frac{8}{25} T_1 T_2] + U_0[T_1^2 T_2^2 + T_2^2 T_3^2 + T_3^2 T_1^2] \} \}, \quad (10)$$

where $j_\ell(x)$ is a spherical Bessel function and we have defined

$$\tilde{r}_1 = |\mathbf{r}_1 - \mathbf{r}_2|, \tilde{r}_2 = |\mathbf{r}_2 - \mathbf{r}_3|, \tilde{r}_3 = |\mathbf{r}_3 - \mathbf{r}_1| = \sqrt{\tilde{r}_1^2 + \tilde{r}_2^2 - 2\tilde{r}_1 \tilde{r}_2 x} \quad (11)$$

in terms of the three particle coordinates. The radial and tensor Yukawa functions are given by

$$Y_i = \frac{e^{-\xi \tilde{r}_i}}{\xi \tilde{r}_i} \left(1 - e^{-C\tilde{r}_i^2}\right), \quad T_i = \left(1 + \frac{3}{\xi \tilde{r}_i} + \frac{3}{\xi^2 \tilde{r}_i^2}\right) \frac{e^{-\xi \tilde{r}_i}}{\xi \tilde{r}_i} \left(1 - e^{-C\tilde{r}_i^2}\right)^2, \quad (12)$$

with parameters $\xi = m_\pi c / \hbar$ (involving the average pion mass m_π) and $C = 2.1 \text{ fm}^{-2}$.

In practice we split $V^{(3)}(k, k'; k_F)$ into the two contributions coming from its attractive and repulsive parts,

$$V^{(3)}(k, k'; k_F) = V_{A_{2\pi}}^{(3)}(k, k'; k_F) + V_{U_0}^{(3)}(k, k'; k_F) \quad (13)$$

in an obvious notation. For each k_F value of interest, $V_{A_{2\pi}}^{(3)}(k, k')$ and $V_{U_0}^{(3)}(k, k')$ are calculated by numerical integration, and rows of $k, k', V_{A_{2\pi}}^{(3)}(k, k'), V_{U_0}^{(3)}(k, k')$ values are stored in a k_F -specific file. Eventually the two additive contributions can be read and utilized as separate entities. Thus they can easily be scaled at will during calculations.

The calculation of $V^{(3)}(k, k'; k_F)$ is very time-consuming and so far we have performed it for just a few representative values of k_F . For those values we were then able to calculate Δ_F . Fortunately, the functional behaviour of $\Delta_F(k_F)$ can be accurately fitted to a Gaussian function over most of its range; the feature is exploited in plotting our results as a function of k_F in Fig. 2.

2.3 In-medium effects

As mentioned previously, the single-particle spectrum $\varepsilon(\mathbf{k})$ and the chemical potential μ are assumed known. In principle these quantities should be derived self-consistently for the given Hamiltonian, density, and temperature (zero in the present case). Lacking that, for exploratory purposes one may consider a range of approximations based on collective experience with similar problems in nuclear many-body physics. The most rudimentary assumption corresponds to the non-interacting Fermi gas,

$$\varepsilon_{\mathbf{k}} = \frac{\hbar^2}{2m} + \mathcal{U}, \quad \mu = \varepsilon_{\mathbf{k}_F} \equiv \varepsilon_F, \quad (14)$$

where m is the bare nucleon mass and \mathcal{U} a constant potential. More correctly, we should consider a self-consistent single-particle potential $\mathcal{U}_{\mathbf{k}}$, or to lowest order the BCS equations for quasiparticles with an effective nucleon mass $m^* \neq m$. In Ref. [20], for example, the neutron effective mass in neutron matter at different densities was calculated within a Brueckner-Hartree-Fock approach, first assuming a 2N potential only (Argonne v_{18}) and then assuming an additional 3N interaction. In the present study we consider several choices for m^* , including those from Ref. [20].

Given the strong short-range repulsions present in the Hamiltonian, we should also be concerned with the presence of short-range correlations, in particular those between the third, unpaired particle and the paired ones in the proper evaluation

of $V(k, k', k'')$. (Such correlations between the paired particles themselves, induced by the inner repulsion of AV18, are taken care of to a certain degree in the trial ground state itself, sufficient to avoid singular behavior [37].) To account for this specific correlation induced by the 3N interaction, we simply introduce a defect function, essentially a Jastrow correlation factor of gaussian type,

$$g(\mathbf{r}) = \exp\{-r^2/b^2\}, \quad (15)$$

which suppresses the contribution of the repulsive component of the 3N potential whenever the third, unpaired nucleon comes close to its paired neighbors. The 3N potential $V_3(\mathbf{r}_1, \mathbf{r}_2, \mathbf{r}_3)$ in coordinate space is then replaced by

$$\tilde{V}_3(\mathbf{r}_1, \mathbf{r}_2, \mathbf{r}_3) = V_3(\mathbf{r}_1, \mathbf{r}_2, \mathbf{r}_3)[1 - g(\tilde{r}_2)]^2[1 - g(\tilde{r}_3)]^2, \quad (16)$$

with \tilde{r}_i defined in Eq. (11). This substitution is straightforward to implement in the calculation of the contribution of the 3N potential to the gap equation, just by inserting the factor $[1 - g(\tilde{r}_3)]^2[1 - g(\tilde{r}_2)]^2$ into the integral in Eq. (10).

In our numerical studies, the values 0.6 and 0.8 fm are considered for the range b of the correlations, (k_F, b) -specific files being created for storing $V_{A_2\pi}^{(3)}$ and $V_{U_0}^{(3)}$.

2.4 Baseline results

In Fig. 1 we show results for the Fermi-surface pairing gap in the triplet $T = 1$ channel as calculated with the AV18 interaction alone. Comparison of the two solid lines demonstrates the effect of introducing the coupling between the P and F channels on the angle-averaged gap: At the peak position ($k_F \approx 2.1 \text{ fm}^{-1}$) the gap is more than tripled. In this case we have considered an effective nucleon mass equal to the bare mass, $m^* = m$. Our results agree with independent calculations in the literature, thus validating the numerical implementation.

If we take into account the in-medium modification of the nucleon mass, the effect of the coupling is moderated substantially, as comparison of the dashed and dot-dashed lines in Fig. 1 shows. For these calculations the values of the effective mass in neutron matter as a function of the Fermi momentum were taken from Ref. [20] (two-body case).

Next we turn to our main subject, the effect of the 3N force combined with in-medium effects on the pairing gap. We will consider only the uncoupled 3P_2 problem at present. This case will suffice for demonstrating the sensitivity of the results to the parameters chosen. The additional effect of PF coupling will be the subject of a future investigation.

3 Tracking the effect of the three-nucleon force

3.1 Scaling the three-nucleon force

First we replicate the results of Ref. [30] for the UIX potential. At this point we should again stress that different parameterizations have been used in the literature in solving the BCS equations: The original one was tuned to the triton binding

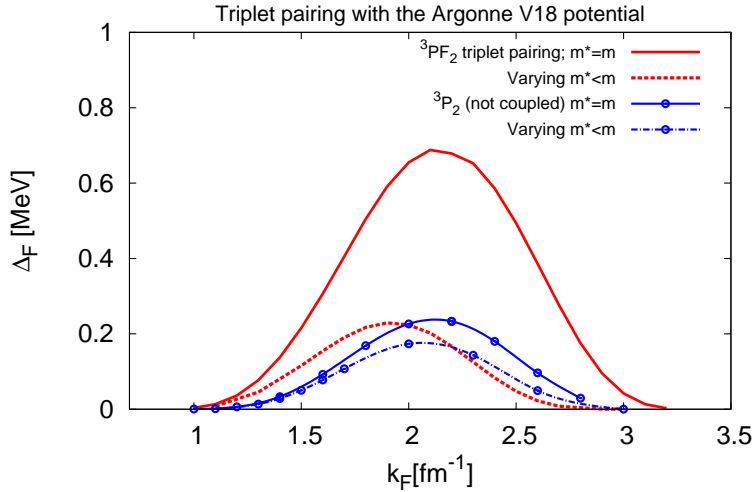


Fig. 1 Pairing gap in the triplet channel as a function of Fermi momentum k_F assuming a bare nucleon mass (*solid lines*) or an effective mass adopted from Ref. [20] (*broken lines*). Results for the coupled 3P_F_2 channel (*solid and dashed red*) are compared with results for the uncoupled 3P_2 channel (*solid with points and dash-dotted blue*). (Color figure online.)

| | original | modified |
|------------|----------|----------|
| $A_{2\pi}$ | -0.0293 | -0.0333 |
| U_0 | 0.0048 | 0.00038 |

Table 1 Coupling constants, in units of MeV, of the original and modified parameterizations of the Urbana IX potential.

energy and the saturation point of nuclear matter within variational CBF theory. A modified parameterization was employed by the Catania/Lanzhou group, readjusted to describe the saturation point within BHF theory [22]. The two sets of parameters are given in Table 1. The attractive part of the modified UIX is 14% stronger than the original value, while the modified repulsive part is one order of magnitude weaker than the original one. Overall, the modified potential is much less repulsive.

In agreement with Ref. [30], we found that if the original UIX force is used, there is no positive solution for the gap: $\Delta_F(k) \equiv 0$. The modified UIX interaction does not produce such dramatic behavior. Representative results will be discussed below. It turns out that the strength of the repulsive term represented by U_0 is a crucial factor. In Fig. 2, we show results obtained by neglecting the U_0 term and compare them with the results with no 3N force present: the gap increases strongly. On the other hand, setting U_0 to half its original value, namely to 0.0024 MeV, leads to a very strong reduction of the gap. It is thus quite revealing to track the behavior of the gap value as the strength of the overall UIX force or separately its repulsive vs. attractive component is varied.

We do so first in Fig. 3 for four representative values of k_F , as indicated, and for different relative strengths $z_u = -U_0/A_{2\pi}^{\text{original}}$. As we gradually turn on the

original 3N UIX interaction (cf. $z_u = 1$ lines), the gap drops somewhat, and after a dramatic discontinuity it vanishes. The results with the original UIX interaction fully turned on are indicated with circles. For $k_F = 3.0 \text{ fm}^{-1}$, the gap vanishes already for a very weak 3N force. If we now neglect the U_0 term (cf. $z_u = 0$ lines), the gap in fact increases, as anticipated already from the comparison in Fig. 2. For values of U_0 in between, the behavior again depends strongly on the details. We attempt to elucidate the origin of the discontinuity in Sec. 3.3.

Figure 3 includes results corresponding to the modified UIX parameters ($z_u = 0.07$). As we turn on the modified UIX force, the results trace the blue dashed lines. The results with the modified UIX fully turned on are indicated with squares. We observe that the modified UIX parameters are such that the inclusion of all, part, or none of it has a very weak influence on the gap in the uncoupled 3P_2 channel.

3.2 In-medium effects

Above we have considered a Fermi-gas single-particle spectrum for the energy $\varepsilon(\mathbf{k}')$ entering the denominator of the gap equation (2), with no modification of the nucleon mass in the medium. Let us now take into account a reduction of the nucleon effective mass, as per the results of Ref. [20], determined both with and without a 3N interaction, i.e., $m^*/m = 0.82$ and 0.86 , respectively. We now consider the solutions of the BCS equations upon replacing m with m^* . For this we focus on the near-peak solution, setting $k_F = 2 \text{ fm}^{-1}$.

Keeping $A_{2\pi}$ fixed at its original or modified value, Fig. 4 tracks the variation of the gap as the repulsive term U_0 is turned on for different m^*/m values. As in the 2N-force results of Fig. 1 for the uncoupled 3P_2 channel, it is found that the influence of the effective mass is quite weak. Again we notice that the modified UIX potential has the curious effect of making the 3P_2 gap almost insensitive to the inclusion of the 3N force. Whether this result originates in deeper consistency relations of the theories involved or is simply fortuitous is an open question. In Sec. 3.3 we will return to this point when discussing the functional form of the total potential.

The 3N force of the Urbana form can be strongly repulsive at short distances and hence may require careful treatment of short-range correlations. To account for this effect, we simply introduce a defect function as explained in Sec. 2. For the range b we consider the values 0.6 and 0.8 fm .

Results obtained with this simple procedure and for the original value of $A_{2\pi}$ are shown in Fig. 5 as a function of U_0 (dash-dotted lines). For comparison and reference, the figure includes results from Fig. 4, and for clarity it zooms in on the domain of U_0 values for which the new results do not vanish. We observe that for small values of U_0 the effect of the correlations is rather weak. Qualitatively, the main effect is the elimination of the discontinuity. Already for small values of U_0 compared to its original value, the gap vanishes.

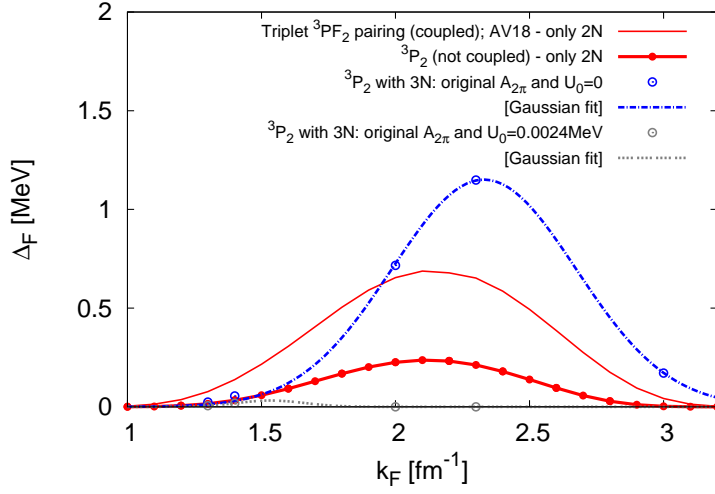


Fig. 2 Pairing gap in the triplet channel as a function of Fermi momentum k_F assuming a bare nucleon mass and different possibilities for the 3N force: (i) not included (*red solid line with points*), (ii) including the original value for the UIX potential $A_{2\pi} = -0.0293$ MeV and setting U_0 to zero (*blue dash-dotted line*) or to $U_0 = 0.0024$ MeV, i.e., half its original value (*grey dotted line*). The open circles correspond to numerical results; dotted and dashed-dotted lines were generated from fitting to those results. (Color figure online.)

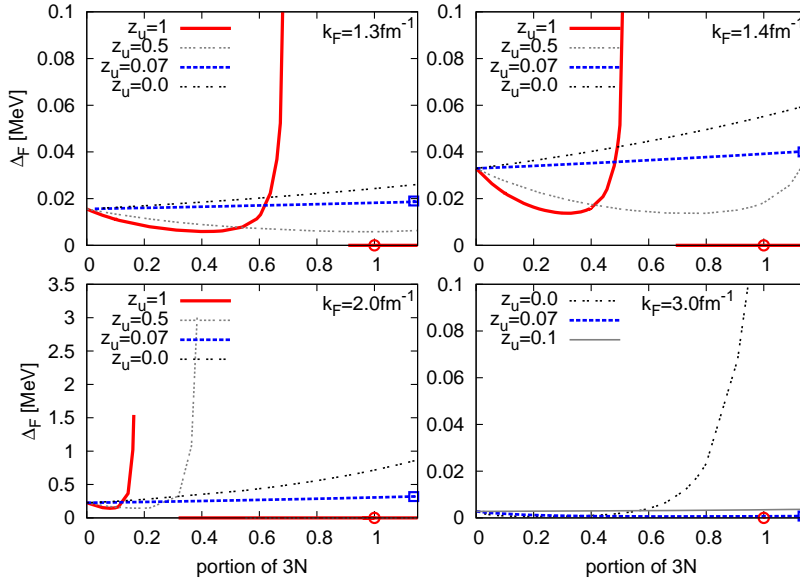


Fig. 3 Variation of the 3P_2 pairing gap with the strength of (i) the 3N Urbana-type force and of (ii) the relative strengths of its repulsive and attractive components, for the indicated values of k_F . The coupling constant $A_{2\pi}$ is scaled by the factor on the x-axis. The ratio $U_0/A_{2\pi}^{\text{original}}$ is further scaled by the factor $z_u \leq 1$. The original UIX potential corresponds to the portion of the 3N force equal to 1 and to $z_u = 1$. The modified UIX potential corresponds to a portion of the 3N force equal to 1.1365 and $z_u = 0.07$ (round points). (Color figure online.)

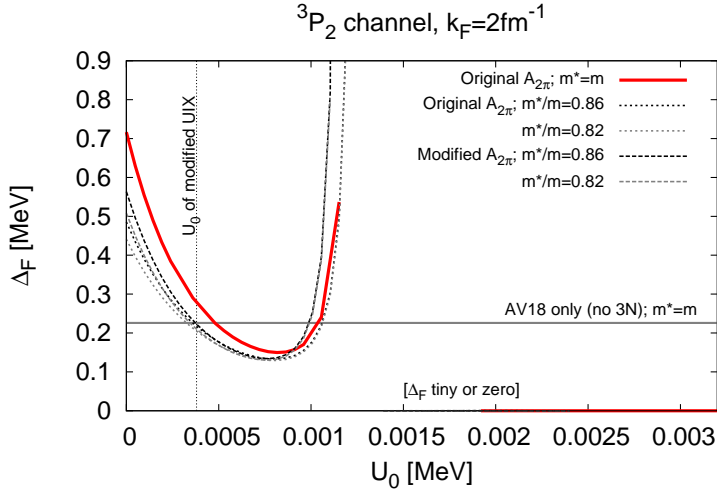


Fig. 4 Pairing gap in the 3P_2 channel in neutron matter for $k_F = 2 \text{ fm}^{-1}$, calculated with the Argonne v_{18} two-nucleon potential and an Urbana-type three-nucleon potential of varying strength, assuming different values for the nucleon effective mass. The original and modified UIX parameters are given in Table 1. (Color figure online.)

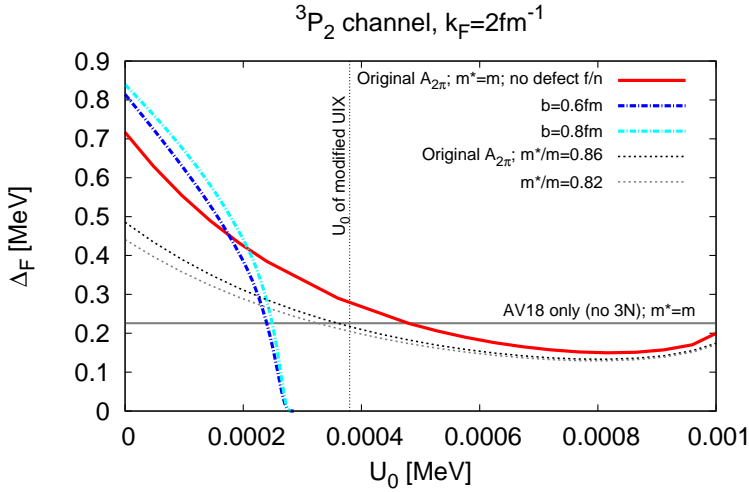


Fig. 5 Pairing gap in the 3P_2 channel in neutron matter at $k_F = 2 \text{ fm}^{-1}$, calculated with the Argonne v_{18} two-nucleon potential and a three-nucleon potential of Urbana IX type with the original attractive part and a varying repulsive strength (cf. Fig. 4), screened by a defect function. The gap is shown as a function of the coupling constant U_0 of the repulsive component. (Color figure online.)

3.3 The role of $V(k, k_F)$

To a large extent, the qualitative differences among the results obtained with the different implementations of 3N potentials can be traced back to the functional form of the potential itself. To clarify this point, we plot in Fig. 6 the 2N AV18 pairing potential $V(k, k_F)$ along with different possibilities we have considered for the 3N contribution $V^{(3)}(k, k_F)$ of Eq. (9), in the representative case $k_F = 2 \text{ fm}^{-1}$. Specifically, for $V^{(3)}$ we have considered (i) the original UIX potential, (ii) the original UIX potential together with a defect function having range $\beta = 0.6$ or 0.8 fm , and (iii) the modified UIX potential. (See Eqs. (9), (13), (16), and Table 1.) First, we note that the main contributions to the integrals in Eqs. (6) and (7) come from the neighborhood of $k' \approx k_F$. It is then readily seen that Eq. (7) generally has no solution if $V_F > 0$. One may also note that the modified UIX potential is negative around $k_F = 2 \text{ fm}^{-1}$, thus enhancing the attraction contributed by the AV18 potential. The original UIX potential, on the other hand, yields an overwhelmingly repulsive contribution, even when a defect function is introduced. In order for the AV18 potential to compensate for the repulsion of the original UIX potential, the latter must be scaled by a factor $|V^{(AV18)}(k_F)|/V^{(3)}(k_F) \approx 0.2$. This is in line with what we observe in Fig. 3: the gap at $k_F = 2.0 \text{ fm}^{-1}$ is finite as long as the 3N contribution is scaled by less than 0.2. As the scaling factor for UIX approaches that critical value from below, i.e., as V_F approaches zero from below, only a very large value of Δ_F can ensure a solution of Eq. (7) – hence the steep rise in Δ_F . Once V_F turns positive, no solution is possible.

In the case where a defect function is introduced, we infer from Fig. 6 that, depending on β , a scaling factor between 0.5 and 1.0 would ensure a negative V_F for $k_F \approx 2 \text{ fm}^{-1}$. We may also infer from the individual parameter values ($V_F^{(A_{2\pi})} = -2.7, -0.3 \text{ MeV fm}^3$) and ($V_F^{(U_0)} = 13.9, 7.5 \text{ MeV fm}^3$) for ($\beta = 0.6, 0.8 \text{ fm}$), respectively, that a value of U_0 scaled by a factor 0.6 to 0.8 relative to the original value could make the overall potential repulsive and kill the gap for $k_F \approx 2 \text{ fm}^{-1}$. As we observe in Fig. 5, the gap vanishes smoothly for a lower scaling factor, i.e., before such a critical value of V_F is reached; hence the disappearance of the discontinuity.

In closing, we may remark that the modified UIX potential seems to act as a small correction to the AV18 potential. This is certainly not the case for the original UIX potential, even if we take into account certain in-medium effects.

4 Summary and perspectives

When exploring the nature of pairing phenomena in dense nuclear matter as it is likely to be present in the hadronic region of neutron star cores, the irreducible three-nucleon interaction cannot be ignored. Yet our knowledge of this interaction, as constrained by empirical data, is quite uncertain. The problem is aggravated by inconsistencies in competing microscopic many-body methods, which have never been tested at the highest densities involved. Consequently, the very existence of a triplet- P pairing gap cannot be decided by theory at this point. Hopefully, vital clues can be gleaned from the growing body of relevant evidence from cooling curves of young neutron stars.

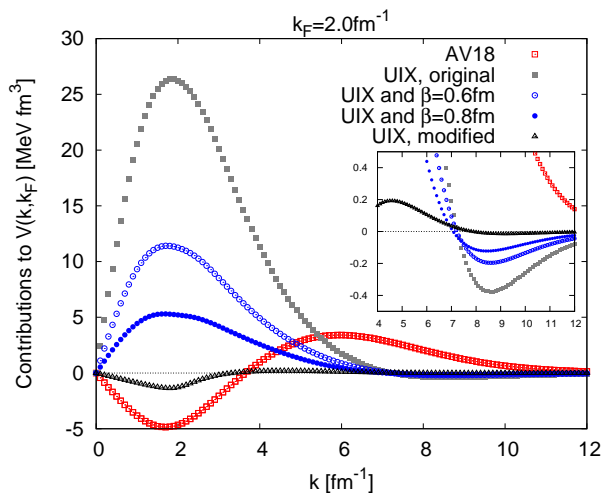


Fig. 6 Contributions to the total $V(k, k' = k_F)$ entering the gap equations in the 3P_2 channel, coming from the pure 2N AV18 potential and from variants of the 3N potential used in this work. (Color figure online.)

The situation described above emerged very clearly in the present study, wherein the gap equation for the triplet- P channel in neutron matter was solved for the AV18 two-nucleon potential and two alternative UIX three-nucleon interactions. We have shown that two parameterizations of the Urbana 3N force, both consistent with empirical saturation properties of nuclear matter within generally accepted many-body computational methods, are likely to give conflicting answers to the binary question of whether there is a finite triplet- P gap. We have shown that a small fraction of the phenomenological repulsion of the original UIX interaction suffices to kill the gap and that the introduction of short-range correlations does not guarantee reversal of this behavior. We cannot exclude the possibility that a special, even pathological, feature of the Urbana-type potential is responsible for our findings. Accordingly, we intend to investigate this issue of the existence of triplet- P pairing for a broader selection of proposed 3N interactions. It also remains to be seen whether the inclusion of coupling to the F channel affects the conclusions drawn from the present study. In particular, it is important to determine whether the sensitivity to the precise treatment of the 3N force persists for other candidate interactions. At any rate, systematic and consistent studies are needed. Their implications will lead to more meaningful comparisons with observational data and to a more profound understanding of nucleonic dynamics in the nuclear medium.

Acknowledgements The work of PP is supported by the Rare Isotope Science Project of the Institute for Basic Science, funded by the Ministry of Science, ICT and Future Planning and the National Research Foundation (NRF) of Korea (2013M7A1A1075764). JWC is pleased to acknowledge research support from the McDonnell Center for the Space Sciences. He is also grateful to the University of Madeira and its Center for Mathematical sciences for gracious hospitality during periods of extended residence.

References

1. D. J. Dean, M. Hjorth-Jensen, *Rev. Mod. Phys.* **75**, 607 (2003). DOI 10.1103/RevModPhys.75.607
2. L. B. Leinson, *Phys. Lett. B* **741**, 87 (2015) DOI <http://dx.doi.org/10.1016/j.physletb.2014.12.017>
3. Ø. Elgarøy, L. Engvik, M. Hjorth-Jensen, E. Osnes, *Nuclear Physics A* **607**(4), 425 (1996) DOI [http://dx.doi.org/10.1016/0375-9474\(96\)00217-5](http://dx.doi.org/10.1016/0375-9474(96)00217-5).
4. C. Schaab, D. Voskresensky, A. D. Sedrakian, F. Weber, M. K. Weigel, *Astron. Astrophys.* **321**, 591 (1997)
5. D. Page, J. M. Lattimer, M. Prakash, A. W. Steiner, in *Novel Superfluids*, Vol. 2, ed. K. H. Bennemann, J. B. Ketterson (Oxford University Press, Oxford, 2014)
6. A. Gezerlis, C. J. Pethick, A. Schwenk, in *Novel Superfluids*, Vol. 2, ed. K. H. Bennemann, J. B. Ketterson (Oxford University Press, Oxford, 2014)
7. J. W. Clark, in *Fifty Years of Nuclear BCS Theory*, eds. R. Broglia, V. Zelevinsky (World Scientific, Singapore, 2013), Chapter 7
8. G. E. Pavlou, E. Mavrommatis, C. Moustakidis, J. W. Clark, *Eur. J. Phys. A*, **53**, 96 (2017), arXiv: **1612.02188** (2016).
9. R. Tamagaki, *Prog. Theor. Phys.* **44**, 905 (1970)
10. T. Takatsuka, R. Tamagaki, *Prog. Theor. Phys.* **46**, 114 (1971)
11. T. Takatsuka, *Prog. Theor. Phys.* **48**, 1517 (1972); *ibid.* **50**, 1754 (1973); *ibid.* **50**, 1755 (1973); *ibid.* **71**, 1432 (1984)
12. L. Amundsen, E. Østgaard, *Nucl. Phys. A* **442**, 163 (1985)
13. M. Baldo, J. Cugnon, A. Lejeune, U. Lombardo, *Nucl. Phys. A* **536**, 349 (1992)
14. T. Takatsuka, R. Tamagaki, *Prog. Theor. Phys. Suppl.* **112**, 27 (1993)
15. M. Baldo, Ø. Elgarøy, L. Engvik, M. Hjorth-Jensen, H.-J. Schulze, *Phys. Rev. C* **58**, 1921 (1998)
16. V. A. Khodel, V. V. Khodel, J. W. Clark, *Phys. Rev. Lett.* **81**, 3828 (1998)
17. V. V. Khodel, V. A. Khodel, J. W. Clark, *Nucl. Phys. A* **679**, 827 (2001)
18. V. A. Khodel, J. W. Clark, M. V. Zverev, *Phys. Rev. Lett.* **87**, 031103 (2001)
19. M. V. Zverev, J. W. Clark, V. A. Khodel, *Nucl. Phys. A* **720**, 20-42 (2003)
20. W. Zuo, C. X. Cui, U. Lombardo, H.-J. Schulze, *Phys. Rev. C* **78**, 015805 (2008) DOI 10.1103/PhysRevC.78.015805
21. B. S. Pudliner, V. R. Pandharipande, J. Carlson, S. C. Pieper, R. B. Wiringa, *Phys. Rev. C* **56**, 1720 (1997)
22. X.R. Zhou, G.F. Burgio, U. Lombardo, H.-J. Schulze, W. Zuo, *Phys. Rev. C* **69**, 018801 (2004) DOI 10.1103/PhysRevC.69.018801
23. J. M. Dong, U. Lombardo, W. Zuo, *Phys. Rev. C* **87**, 062801 (2013). DOI 10.1103/PhysRevC.87.062801
24. Z. H. Li, U. Lombardo, H.-J. Schulze, W. Zuo, *Phys. Rev. C* **77**, 034316 (2008) DOI 10.1103/PhysRevC.77.034316.
25. S. Maurizio, J. W. Holt, P. Finelli, *Phys. Rev. C* **90**, 044003 (2014). DOI 10.1103/PhysRevC.90.044003
26. J. Bardeen, L. N. Cooper, J. R. Schrieffer, *Phys. Rev.* **108**, 1175 (1957)
27. R. Balian, N. R. Werthamer, *Phys. Rev.* **131**, 1553 (1963)

-
28. E. Krotscheck, J. W. Clark, Nucl. Phys. A **333**, 77 (1980)
 29. P. Grangé, A. Lejeune, M. Martzloff, J. F. Mathiot, Phys. Rev. C **40**, 1040 (1989) DOI 10.1103/PhysRevC.40.1040.
 30. L. Yuan, Ph.D. Thesis, Washington University (2007)
 31. A. Akmal, V. R. Pandharipande, D. G. Ravenhall, Phys. Rev. C **58**, 1804 (1998)
 32. P. B. Demorest, T. Pennucci, S. M. Ransom, M. S. E. Roberts, J. W. T. Hessels, Nature **467**(7319), 1081 (2010)
 33. J. Antoniadis, et al., Science **340**(6131) (2013). DOI 10.1126/science.1233232
 34. A. W. Steiner, J. M. Lattimer, E. F. Brown, Ap. J. **722**(1), 33 (2010)
 35. V. A. Khodel, V. V. Khodel, J. W. Clark, Nucl. Phys. A **598**, 390 (1996)
 36. X.-R. Zhou, H.-J. Schulze, E.-G. Zhao, F. Pan, J. P. Draayer, Phys. Rev. C **70**, 048802 (2004)
 37. L. N. Cooper, R. L. Mills, and A. M. Sessler, Phys. Rev. **114**, 1377 (1959)